Title
Utilizing crosswell, single well and pressure transient tests for characterizing fractured gas reservoirs

Journal
The Leading Edge, 15(8)

ISSN
1070-485X

Authors
Majer, EL
Datta-Gupta, A
Peterson, JE
et al.

Publication Date
1996-08-01

DOI
10.1190/1.1437401

Peer reviewed

Utilizing crosswell, single well and pressure transient tests for characterizing fractured gas reservoirs

E. L. MAJER, A. DATTA-GUPTA, J. E. PETERSON, D. W. VASCO, L. R. MYER, T. M. DALEY and B. KAELIN
Center for Computation Seismology Earth Sciences Division
Ernest Orlando Lawrence Berkeley National Laboratory
Berkeley, California

J. QUEEN, P. S. D'ONFRO, W. D. RIZER, D. COX, and J. SINTON
Conoco Inc.
Ponca City, Oklahoma

As part of its Department of Energy (DOE)/Industry cooperative program in oil and gas, Berkeley Lab has an ongoing effort in cooperation with Conoco and Amoco to develop equipment, field techniques, and interpretational methods to further the practice of characterizing naturally fractured, heterogeneous reservoirs. The focus of the project is an interdisciplinary approach, involving geology, rock physics, geophysics, and reservoir engineering. The goal is to combine the various methods into a unified approach for predicting fluid migration.

During the last five years a series of joint LBL/Conoco/Amoco seismic and well-test field experiments have been conducted at Conoco's Newkirk, Oklahoma Borehole Test Facility (Figure 1). The facility contains six deep and five shallow wells used for geophysical and hydrological tests. The site occupied for the subject experiments consists of the five shallow groundwater wells (GW) in a "5-spot" pattern with the outside wells approximately 50 m from the center well. The shallow wells penetrate a fractured shale and limestone sequence of the Lower Permian Chase Group. The regional dip of the formations is less than 1" west-southwest. Two orthogonal sets of vertical fractures have been mapped from a nearby surface exposure of the limestone: a systematic set striking north 70" east and a nonsystematic set at north 25°west. The velocity variations between the shale and the limestone at this site are sizable: contrasts of 2 to 1 exist.

Figure 2, a velocity log derived from the single well data in well GW-3, shows the strong velocity variation between the shale above and below the high velocity Fort Riley Limestone. This velocity contrast also indicates a general contrast in the physical properties, i.e. possibly in the transport properties as well. The work described in this paper is focused on

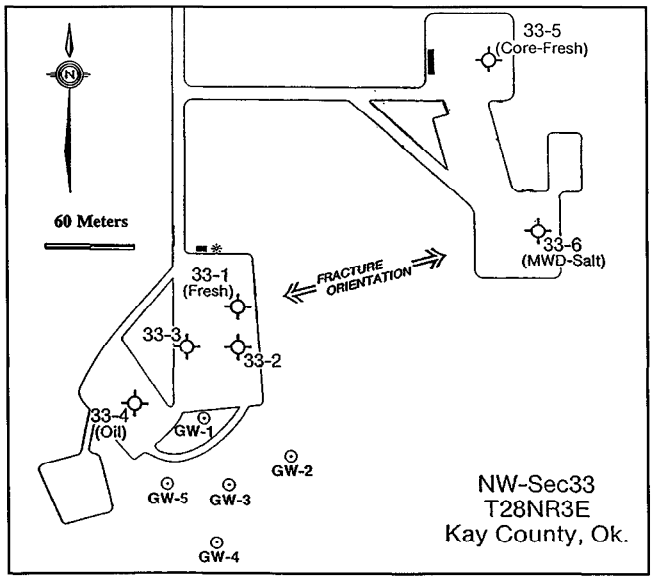

Figure 1. Plan view of the Conoco borehole test facility near Newkirk, Oklahoma, showing the geometry of the wells used (the GW wells) and the predominant fracture direction as inferred from mapping nearby outcrops of the limestone formation in which the seismic imaging was performed.

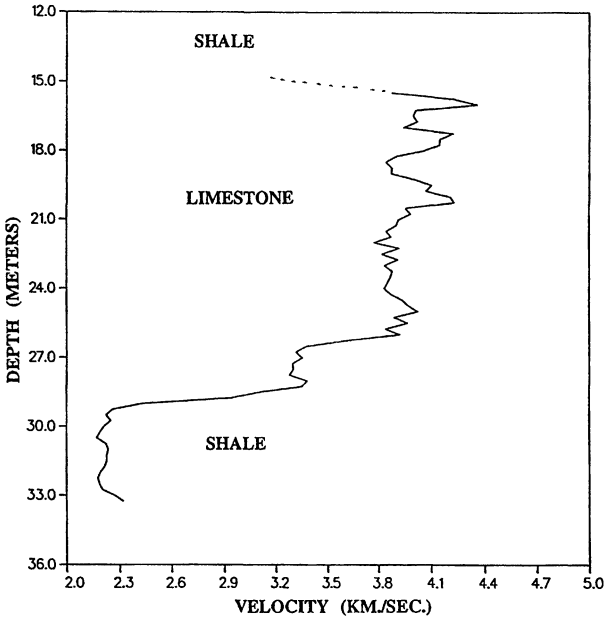

Figure 2. P-wave velocity log as a function of depth in well GW-3 as derived from the near-offset data in the single well survey. The single well and crosswell measurements were carried out over the 15-30 m depth range.

the Fort Riley Limestone, a 10- 15-m thick fractured formation approximately 15 meters below the surface.

Previous crosswell and hydrologic tests are strong evidence of open and conductive fractures trending north 70" east. Specifically, the pump tests showed that wells GW-5 and GW-2 seemed to be connected by a "fast path"; however wells GW-3,4 and 1 were not as well connected to each other, or to GW-5 and 2. Also previous seismic work (VSP and earlier crosshole in the GW wells) indicated seismic anisotropy consistent with the mapped fracture direction of north 70" east.

Figure 3 shows two different realizations of inverting the data from the pump tests in the GW wells. Figure 3a is the result of taking the ensemble median of discontinuum models. The discontinuum models are obtained by randomly selecting elements and turning them on and off to minimize the difference between computed and observed values of drawdown data from the pump tests. Figure 3b shows the result of taking the median of the variable-aperture lattice models based on a parallel plate concept, using aperture instead of fracture conductivities. Figure 3 shows a conductive feature approximately parallel to a line extending from GW-2 to GW-5, between GW-1 and GW-3 with a mean aperture of 0.65 cm.

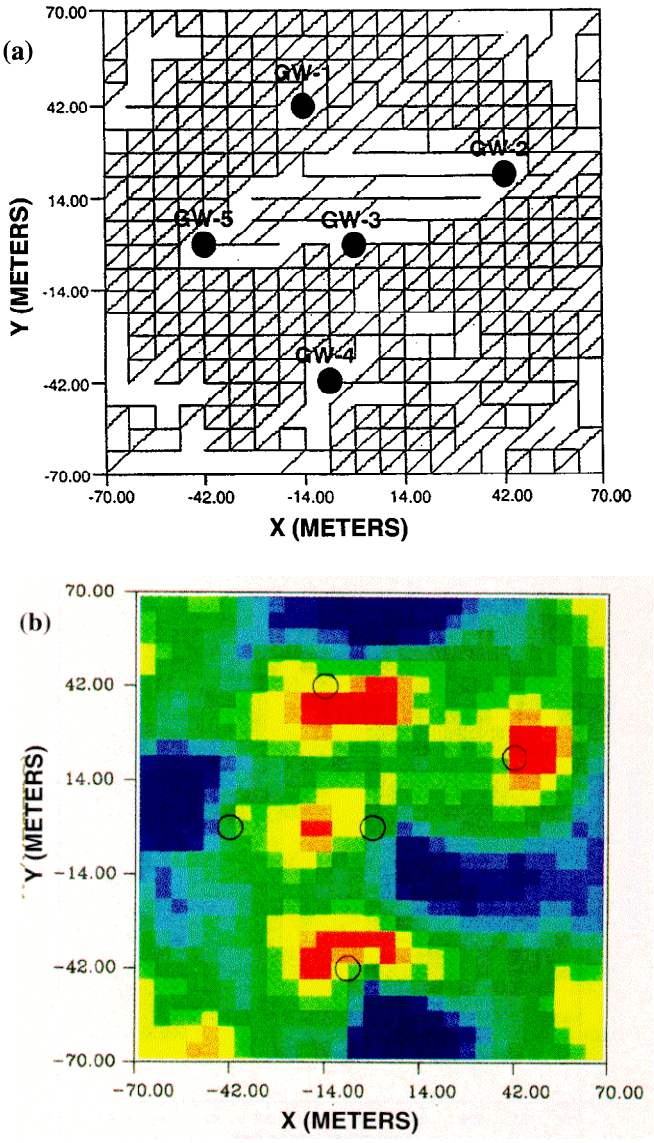

Figure 3. Result of inverting the well test data in the GW-well field. (a) Result of using a discontinuum model using triangular grids, and (b) ensemble median model using the variable-aperture lattice approach. Both inversion models indicate a connected path between GW-5 and GW-2.

In addition to the seismic and hydrologic evidence for a fast path fracture system between GW-2 and GW-5, core from GW-5 indicated vertical fracturing in the lower part of the Fort Riley Limestone. That is, the dominant fracture direction inferred from the initial seismic and hydrologic data was consistent with the stress and geologic interpretation from previous studies in the area.

In order to enhance the seismic visibility of the suspected fracture, or fracture system, we decided to inject air into the formation with the assumption that the air would travel in the permeable feature and increase the reflectivity, and/or attenuation properties of the fractures. The plan was to inject air into GW-5 and draw down GW-2 below the Fort Riley Formation.

Field experiment. In June 1994, air was injected into the Fort Riley Limestone between packers placed in well GW-5. The concept was to perform before, during and after seismic imaging experiments to determine the effect of air injection. Care was taken to keep air injected pressure below the parting pressure of the formation. During the air injection a pump was placed at the bottom of GW-2 to keep the water level below the bottom of the limestone. This would create a negative pressure gradient in GW-2 and further encourage flow of the air towards it.

Before the air was injected, a series of crosswell measurements was taken between the center well and each of the outer GW wells. The crosswell survey used a piezoelectric source (cylindrical bender) with a swept sine wave using frequencies from 1000-10 000 Hz over a 50-ms time window, and a recording time of 80 ms at 50 000 samples/s. A 16-bit, 12-channel system was used, capable of recording 100 000 samples/s per channel, including power electronics developed at Berkeley Lab to deliver up to 8000 volts peak to peak at several amps into a cable of up to 1 microfarad capacitance from 500- 15 000 Hz.

Also, single well reflection surveys were performed in wells GW-1 and GW-3, by hanging the S-element hydrophone string with 1/4-m intervals in the same well as the source. As the string of receivers was held in place, the source was moved from one meter below the bottom receiver to the approximate bottom of the Fort Riley Formation at 1/4-m intervals. The receiver string was then moved up 1/4-m and the procedure repeated until the entire Fort Riley Formation was covered. These surveys resulted in multifold imaging data sets using a split spread configuration.

The effect of the air injection in well GW-5 was then continuously seismically monitored between GW- 1 and GW-4 by placing the piezoelectric transmitter at the center of the Fort Riley Formation in GW-1 and centering the receiver string in the formation in GW-4 with the eight elements at l-m spacing. The transmitter and receiver string were not moved during this monitoring. After the completion of the air injection, crosswell measurements were again taken between GW-3 and the other four wells.

Seismic monitoring during air injection. The monitoring began 30 minutes before the start of the air injection and was repeated at two-minute intervals. After one hour, when no

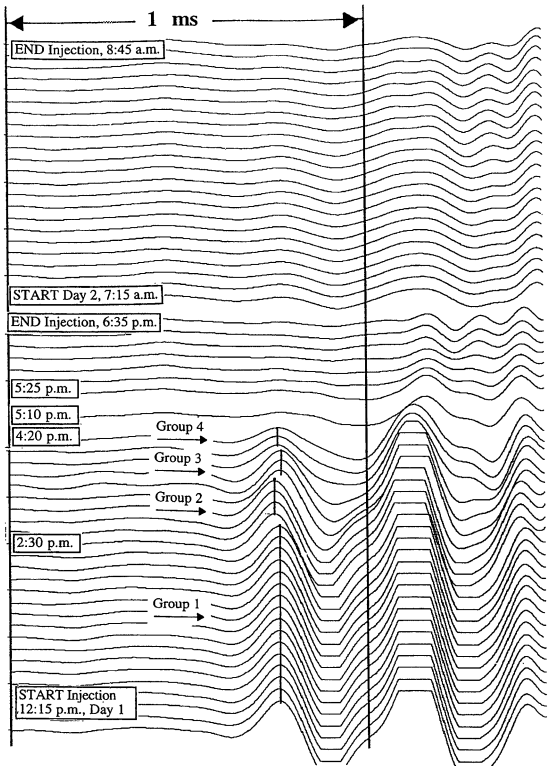

Figure 4. Crosswell seismic data recorded during the air injection between wells GW-4 and GW-1. This figure shows the behavior (attenuation and time delay) of the P-wave data as air is injected into the formation. The amplitude scale is the same for all traces. Time zero is at the bottom of the figure.

change in the signal was observed, monitoring was increased to every 10 minutes. Figure 4 shows the effect of air injection on the crosswell seismic measurements during the injection. It should be noted that all amplitudes are plotted at the same scale. Over time a general decrease in both traveltime and amplitude was observed, with a significant change occurring approximately two hours and 15 minutes after start of air injection (note the shift in traveltime between the set of traces marked group 1 and group 2 in Figure 4). Air injection was stopped when we saw no significant change in the crosswell data. It is obvious from the crosswell data in Figure 4 that the air injection had a large effect on the seismic properties.

Crosswell imaging data analysis. The crosswell results can be quantified by calculating a summed spectral amplitude over a specified frequency band (4000-6000 Hz) in 0.08 ms time steps along each trace at each depth. The resultant time-amplitude plots for each trace are shown in Figure 5 between well pairs GW-3/GW-1 and GW-3/GW-4 before and after air injection. The only significant difference between the before and after data from GW-3 to GW-4, is the increase in amplitude of a secondary arrival at 17 ms. However, a large decrease in seismic energy was observed between GW-3 and GW- 1. This is interpreted as a result of the air being injected into a fracture. Crosswell pairs GW-3-GW-5 and GW-3-GW-2 are similar to GW-3 to GW-1. We assume this is due to effects of air being injected at GW-5, and the water level in GW-2 being drawn down.

The increase in amplitudes at 17 ms between GW-3 and GW-4 is interpreted as a reflection arrival from the vertical fracture set. At 4000 m/s velocity, this would put a vertical feature about 14 meters from GW-3. Using the crosswell

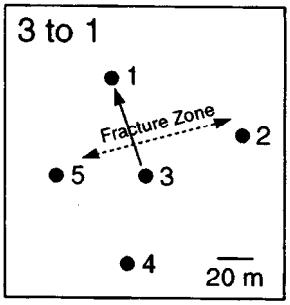

(a) GW-3 to GW-1

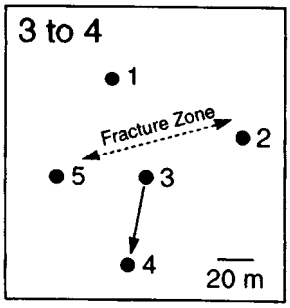

(b) GW-3 to GW-4

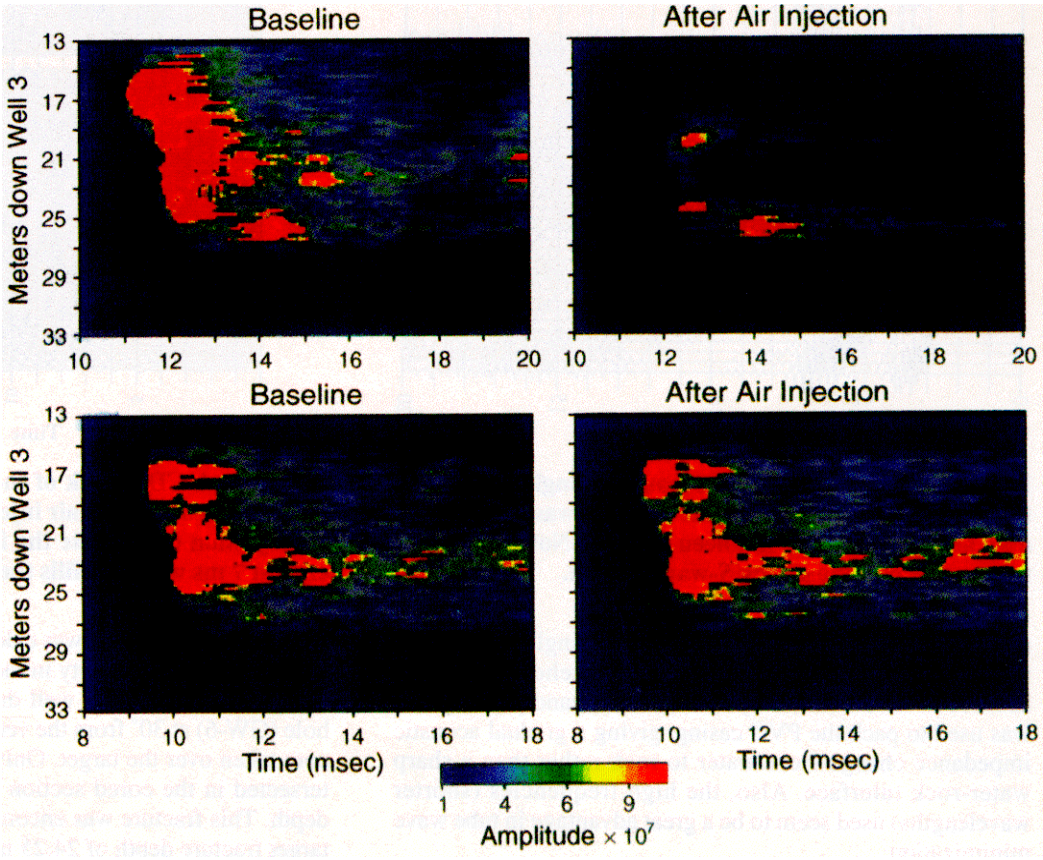

Figure 5. Crosswell amplitude data as a function of depth and time (a) between well pairs GW-3/GW-1, and (b) between wells GW-3/GW-4 before and after air injection.

data alone, the strike of such a feature cannot be determined; the conclusion that there is a fracture between GW–3 and GW–I is based only on the drop in amplitude of the crosswell data between those boreholes.

Single well CDP data. The single well experiment was designed with the intention of processing the data as a common CDP reflection survey. Data were acquired from wells GW–3 and GW–1 before and after the air injection. The data were initially sorted into CDP gathers which showed a low–amplitude ***P-wave*** arrival at 4000 m/s velocity and large–amplitude secondary arrivals at 2200 m/s velocity. Secondary arrivals were interpreted as S–waves, based on the radiation pattern observed in these data which shows maximum energy at 45. to the borehole. Shown in Figure 6 are several shot gathers from the single well profiling, where the strong S–wave arrivals are clearly seen. The data are surprisingly free of tube waves which are commonly seen in borehole data. The absence of tube waves may be due to the sand packing that was used to pack the PVC casing, giving a gradual acoustic impedance change from water to rock rather than a sharp water–rock interface. Also, the high frequencies (shorter wavelengths) used seem to be a great advantage in tube wave minimization.

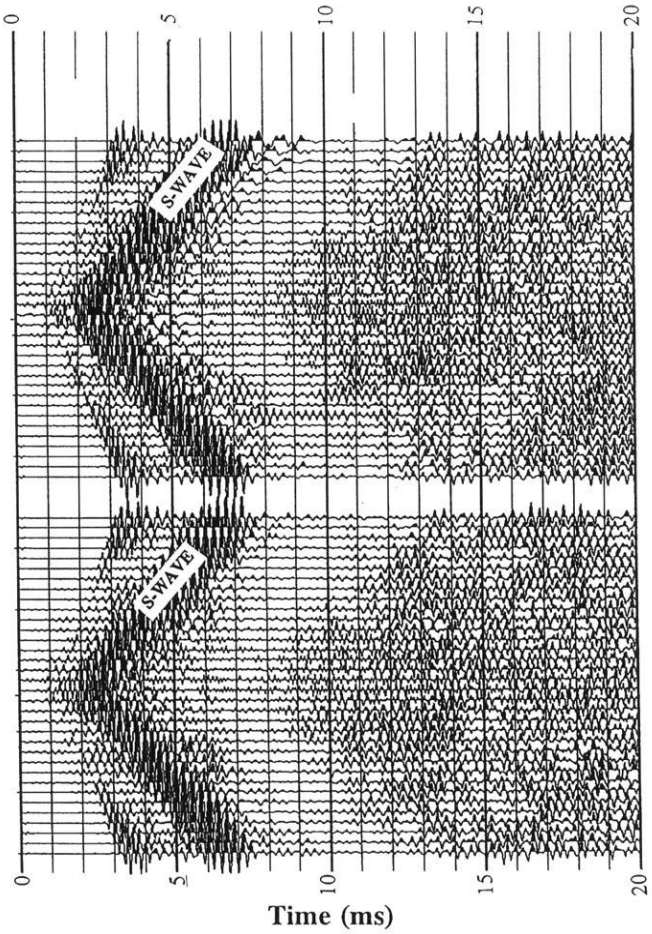

Figure 6. Typical shot gathers from the single well reflection profile in GW-3. Receiver spacing was 1/4-m. The data are raw and have not been filtered. Note the lack of tube waves and the strong S-wave arrival.

The resulting CDP stacks before and after the air injection in GW–3 are shown in Figure 7. The two sections representing before and after injection are almost identical except for a strong reflector at 7 ms after injection. This reflector was observed at the same time as the proposed reflector seen in the GW–3 to GW–4 crosswell data. The reflection is strong from a depth of about 19–26 m, which is a region of relatively high velocity (see Figure 2). The reflector appears to extend to a depth of 28 m with some evidence of reflected energy shallower than 19 meters.

Traveltime between GW–I and GW–3 is about 12.5 ms, and therefore, the reflector seen in Figure 7 at 7 ms should be at 18 ms from before to after injection (Figure 8). However, the reflector appears very weak, probably due to its distance from GW– 1.

Results of drilling. In order to verify our results we designed a drilling program based on the combined results of the single well and crosswell surveys. A target zone in the Fort Riley Limestone was determined at a depth of 24.25 m below the surface, and 13.54 m from GW–3, on a line connecting GW–3 and GW–1. This zone was calculated from the reflection arrival and average velocity in the limestone.

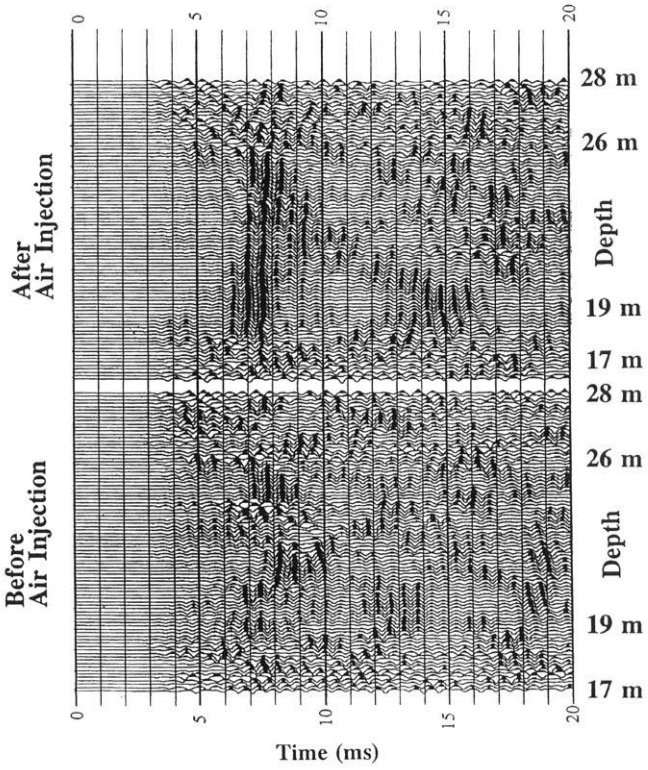

Figure 7. A CDP stack of the single well reflection data from GW-3 before the air injection (bottom) and after the air injection (top). Note the increase in the reflected energy at *7* ms when air fills the fracture zone.

A commercial slant well drilling rig was used to drill a hole (GW–6) at 30° from the vertical into the target zone with core taken over the target. Only one natural fracture was intersected in the cored section between 24.9 m and 25.1 m depth. This fracture was encountered less than 1 m from the target fracture depth of 24.25 m predicted by the single–well

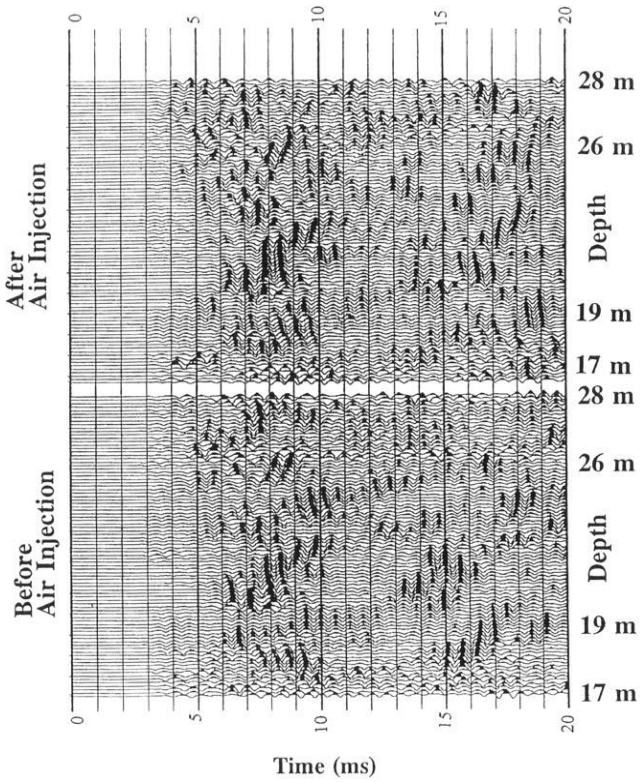

Figure 8. A CDP stack of the single well reflection data from GW-1 before the air injection (bottom) and after the air injection (top). Although there is an increase in the reflected energy between 15 and 18 ms when air fills the fracture zone, the energy is weaker due to the larger distance the fracture is from GW-1 than GW-3.

and crosswell seismic experiments. A photograph of the cored fracture is shown in Figure 9.

There are three pieces of evidence that suggest the fracture is natural and not drilling induced. The fracture is planar and oriented 30° to the core axis (Figure 9). This orientation is consistent with an interpretation that the fracture is vertical. Second, we examined the fracture surface under an optical microscope and observed perfectly formed dog-tooth spar (calcite) and framboidal pyrite. Their occurrence indicates that the fracture was open in the subsurface enabling euhedral mineral crystals to form. Third, the driller noted significant water influx immediately after 24.9 m. This observation is the most compelling evidence that the fracture in the core is natural and the target fracture.

It was impossible to measure the aperture of the natural fracture in GW-6 because one side of the fracture was broken into rubble (Figure 9). However, based on our observations of the natural fracture in the GW-5 core, we estimate that the fracture in GW-6 has an aperture of approximately 1 mm in the subsurface. This estimate is also supported by the interpretation of a tracer survey conducted in the GW well array that suggested a fracture aperture between 0.7 and I.2 mm.

Conclusions. Before this work began we were uncertain that fracturing, or heterogeneity, could be mapped at a fine enough scale with seismic methods to provide useful input to fluid transport models, or for validating these models. Although we by no means claim to have solved the problem, we feel that we have taken a small step towards providing an approach to characterizing fractured heterogeneous environments. As usual there is no one magic method that can solve a difficult problem and one must resort to a combination of approaches. We guided the seismic work by interacting with geologists and reservoir engineers. The primary goal was to develop an effective method for imaging the fractures that are important in controlling fluid transport.

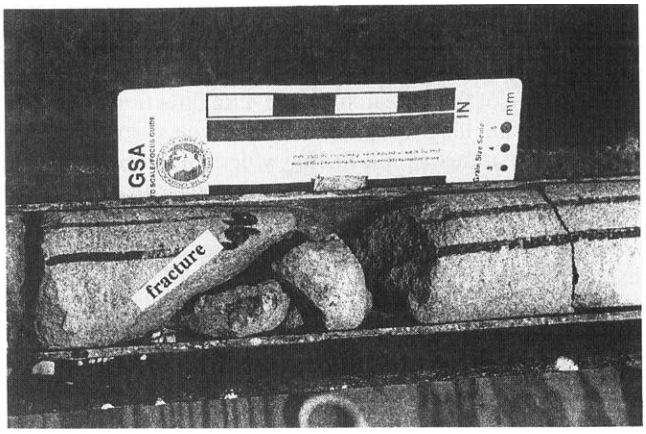

Figure 9. Natural fracture in GW-6 core between 24.9 and 25.1 m depth. The top of the core section is on the left. The core piece on the left has a planar, natural fracture oriented 30° to the core axis. The other side of the fracture has been broken into rubble. The scale is 10.16 cm (4 inches).

We feel that the results from this work prove that:

1) Single well reflection surveys can provide useful information on vertical features a significant distance from the well. Single well surveys hold great promise in characterizing fine scale reservoir heterogeneity, but due to operational issues (tube waves, horizontal velocity gradients, lack of commercial systems) the method has not been extensively used. The single well data presented here were characterized by a lack of tube waves, but contained large shear wave energy. The tube waves may have been attenuated by the sand packing around the boreholes and it must be anticipated that strong tube waves could exist in other single well surveys. We feel that our success was a combination of careful attention to electronic noise reduction, the use of high frequency data, and well conditions. It is difficult to determine the effect strong tube waves would have on the processing, but the shear wave energy was easily removed with f-k filtering.

2) Relatively small fractures can account for significant fluid flow. Methods such as VSP and surface reflection may provide clues to general fracture directions and anisotropy but to accurately locate and characterize such features is a difficult task and requires high resolution subsurface methods. Using standard processing techniques, fracture zones were located which could be detected, but not located, by other means. This was accomplished by utilizing high frequency energy in a combination of crosswell and single well approaches.

3) From a rock physics point of view, we have shown that replacement of water with a gas (in this case air) produces large changes in the P-wave signal, even in such small features as a fracture with a width on the order of a millimeter. This is significant because although our wavelengths were on the

order of one half to one meter, we still "saw" the fracture. This is field evidence in support of the displacement discontinuity theories that predict such effects.

The future of this research is in several directions. We will pursue field and laboratory scale experiments to explain why such small features as millimeter-wide single fractures can cause large seismic anomalies. The next phase of the experiments will be to repeat the crosshole seismic work while "over" inflating the fracture zone and measuring the actual displacement of the fracture where it was intersected by the corehole. Thi.s will provide a quantitative measure of a gas filled fracture versus the seismic properties. We will also observe guided wave behavior along the fracture by performing a crosshole seismic experiment along the fracture between GW-5 and GW-2. Just as importantly, we will next take the high frequency crosshole and single well methods to larger scales with surveys in production scale fields. We feel that only in this joint basic/applied approach can we make true progress in developing useful methods for characterizing heterogeneous reservoirs.

Suggestions for further reading. There have been numerous publications resulting from studies of the seismic anisotropy, principal stress orientations and preferred flow direction in the Fort Riley Limestone at the Conoco Borehole Test Facility. Queen and Rizer's July 1990 paper in the *Journal of Geophysical Research,* "An integrated study of seismic anisotropy and the natural fracture system at the Conoco Borehole Test Facility, Kay County, Oklahoma" was a groundbreaking paper documenting the relation found between the orientations of surface joints and subsurface fractures, the principal stress directions from point load tests and from borehole breakouts, and shear wave polarization azimuth in VSPs. The addition of flow analysis of the system was made by Datta-Gupta et al, as published in "Detailed characterization of a fractured limestone formation by use of stochastic inverse approaches", in SPE *Formation Evaluation,* September 1995. Additional work at the test site by Harlan, 1990, SEG *Expanded Abstracts,* and by Lines et al, 1992, GEOPHYSICS, document the seismic velocities at the Fort Riley Limestone. LE

Acknowledgments: This work was supported by the Assistant Secretary for Fossil Energy, Office of Oil Gas and Shale Technologies, Royal Watts, Program Manager U. S. Department of Energy under Contract No. DE-ACO3-76SFOOO98. We are grateful to Conoco Inc. for their support of this project and to Henry Tan for Amoco's continued support and interest in this work. All computations were carried out at the Centerfor Computational Seismology, the field work was supported by the Geophysical Measurement Facility at the Ernest Orlando Lawrence Berkeley National Laboratory, both supported by DOE's Office of Energy Research Geosciences Program. We would also like to thank Chris Doughty and Jane Long for their input.

Ernest L. Majer received his doctorate in geophysics (1978) from the University of California at Berkeley and is currently department head of subsurface geosciences in the Earth Sciences Division at Ernest Orlando Lawrence Berkeley Lab. Current activities focus on utilizing VSP and tomographic mapping techniques for characterizing geothermal, petroleum, and toxic waste environments. A principal effort is to link hydrologic parameters to seismic properties.